Journal of Materials Science & Nanotechnology
Volume 9 | Issue 1
ISSN: 2348-9812

Research Article Open Access

Microscopic Characteristics of Nanoparticles inside the Liquid Suspension by Molecular Dynamics Simulation

Xu Z[1], Liu J[*1], Zhang X[2] and Yang Y[1]

[1]Key Laboratory of Low Grade Energy Utilization Technology and System, School of Energy and Power Engineering, Chongqing University, Chongqing, 400030, China
[2]School of energy and power engineering, North university of China, Taiyuan, Shanxi, 030051, China

[*]**Corresponding author:** Liu J, Key Laboratory of Low Grade Energy Utilization Technology and System, School of Energy and Power Engineering, Chongqing University, Chongqing, 400030, China, Tel: +086-023-65102473, E-mail: juanfang@cqu.edu.cn

Citation: Xu Z, Liu J, Zhang X, Yang Y (2021) Microscopic Characteristics of Nanoparticles inside the Liquid Suspension by Molecular Dynamics Simulation. J Mater Sci Nanotechnol 9(1): 104

Received Date: February 23, 2021 Accepted Date: May 22, 2021 Published Date: May 24, 2021

Abstract

Conveying nanopowder or nanoparticles are involved in the numerous industry fields, but discontinuous and unstable transportation often takes place, and even the pipes clogged because of nanoparticle aggregation. Understanding in detailed the microscopic characteristics of nanoparticles suspended in the base fluid will play a vital role. Additionally, nitrogen is commonly adopted as a powder carrier fluid due to its strong insert and nonpolar. In the present work, the large-scale molecular dynamics simulation is conducted to explore the movement, distribution, suspension and diffusion of the copper nanoparticles in the nitrogen-based liquid at the atomic level. The effects of the system temperature, the size and volume fraction of the particles on the suspension stability and the aggregation degree are mainly discussed. The influence law of each factor on the microscopic characteristics of the suspension is further identified. Meanwhile, the most stable suspension and the best suitable particle size are found on the different conditions.

The results will provide theoretical guides for the stable transport of the NPs.

Keywords: Molecular dynamics; nanoparticles; liquid suspension; diffusion coefficient, suspension stability

List of abbreviations: COM: Center of Mass; FCC: Face-Centered Cubic; Cu: Copper; LAMMPS: Large-Scale Atomic/Molecular Massively Parallel Simulator; LJ: Lennard-Jones; MDS: Molecular Dynamics Simulation; MSD: Mean Squared Displacement; N: Nitrogen; NP: Nanoparticles; NVT: Constant Volume and Constant Temperature Ensemble; RDF: Radial Distribution Function

Introduction

With the rapid development of nanotechnology, nanopowder or nanoparticles (NPs) have attracted extensive attention due to their special properties, such as the surface effect, scale effect and quantum effect [1-3]. Adding NPs into the fluid can change or maybe enhance the properties of the fluid [4]. However, NPs are prone to aggregation occurring because of their large specific surface area and specific surface energy. Consequently, nanopowder or nanoparticles always stick to the pipe wall, and even the pipes clogged, which make it extremely difficult to continuously convey the NPs [5]. Therefore, understanding deeply the characteristics of nanoparticles suspended in the base fluid will play a vital role in the various fields, such as sediment formation, solid-liquid separation and nanopowder transportation [6,7].

Although there have been numerous researches on the NP properties, most have focused on the nanofluids, which are one special kind of the liquid suspension. In nanofluids, NPs are required to be homogenously distributed in the base fluid. At present, charactering the NPs in the base fluids by aid of the experimental method is still difficult and deficient, and thus the computer modeling, in particular, molecular dynamics simulation (MDS), is considered as one powerful tool. MDS is a deterministic method that involves tracking atomic trajectories by numerically solving the Newton's motion equation based on a specific interatomic potential with certain initial conditions and boundary conditions [8].

NP aggregation is one of the important factors affecting the thermal conductivity of nanofluids [9,10]. For a certain particle density, aggregation can increase the thermal conductivity [11]. The effect of the aggregation type on the thermal conductivity was further analyzed [12]. The mechanism of NP aggregation was also revealed by investigating the microscopic behavior of NPs during the diffusion-limited aggregation [13]. In addition, the NPs in the nanofluid are found to be the fractal objects, and their distribution exhibits the fractal characteristics [14-17]. So the NP aggregation could be represented by the fractal dimension [18,19].

The previous studies have mainly concentrated on the effect of the NP aggregation on the thermophysical properties of nanofluids. Moreover, water or argon was often chosen as the base fluid, in which water is the polar molecule and argon is the monoatomic molecule. However, in fact, liquid N_2 is always adopted as a powder carrier fluid due to its inert and nonpolar. In the present paper, we concentrate on the liquid suspension comprised of Cu nanoparticles and liquid N2. In the literature, no information is available about the characteristics of the Cu-N2 liquid suspension. In the present work, MD simulation is adopted to study the microscopic behavior of the nanoparticle liquid suspension. Furthermore, the key factors controlling the suspension state and stability of the particles in the base fluid are identified. The results will provide theoretical guides for the stable transport of the NPs.

Simulation method

Potential function

In the suspension, Cu nanoparticles are the face-centered cubic (FCC) structure with a cubic side of 3.615 Å, and the liquid N2 molecules are nonpolar, electrically neutral, and treated by the coarse graining. The shifted Lennard-Jones (LJ) potential function was adopted to describe the interaction between the atoms

$$\varphi(r_{ij}) = 4\varepsilon_{ij}\left[\left(\frac{\sigma}{r_{ij}}\right)^{12} - \left(\frac{\sigma}{r_{ij}}\right)^{6}\right], \ (r < r_c) \qquad (1)$$

where ε is the potential well, σ is the atom diameter, r_{ij} is the distance between atom i and atom j, r_c is the cut-off radius and set to be 12 *Å*. The potential parameters of each atom type are listed in Table 1. In which, the parameters of Cu-N were obtained by the Lorentz-Berthelot mixing rule [8]

atom	ε/(kcal. mol^{-1})	σ/Å
N-N	0.2005	3.6231
Cu-Cu	9.4461	2.3377
Cu-N	1.3762	2.9804

Table 1: Parameters of the LJ potential [16,20]

$$\sigma_{\alpha\beta} = \frac{1}{2}\left(\sigma_{\alpha\alpha} + \sigma_{\beta\beta}\right) \quad (2)$$

$$\varepsilon_{\alpha\beta} = \sqrt{\varepsilon_{\alpha\alpha} + \varepsilon_{\beta\beta}} \quad (3)$$

Computational details

The open source large-scale atomic/molecular massively parallel simulator (LAMMPS) is employed in our simulation. The constant volume and constant temperature (NVT) ensemble was used. The system temperature is maintained by using the Nosé-Hoover method. Periodic boundary conditions are imposed in each direction. The time step is 1fs, and each case run 5ns. In which, the first 1ns is utilized to relax and equilibrate the system, and the last 4ns to collect the statistical data. The system is initialized based on the energy minimization principle, and then run at a constant temperature.

We constructed five different suspensions, and the corresponding parameters are given in Table 2. For each liquid suspension, initially two Cu NPs are placed in the system center and separated by 1 nm. One instantaneous configuration of one suspension is presented in Figure 1, in which the two particles are well suspended in the base fluid.

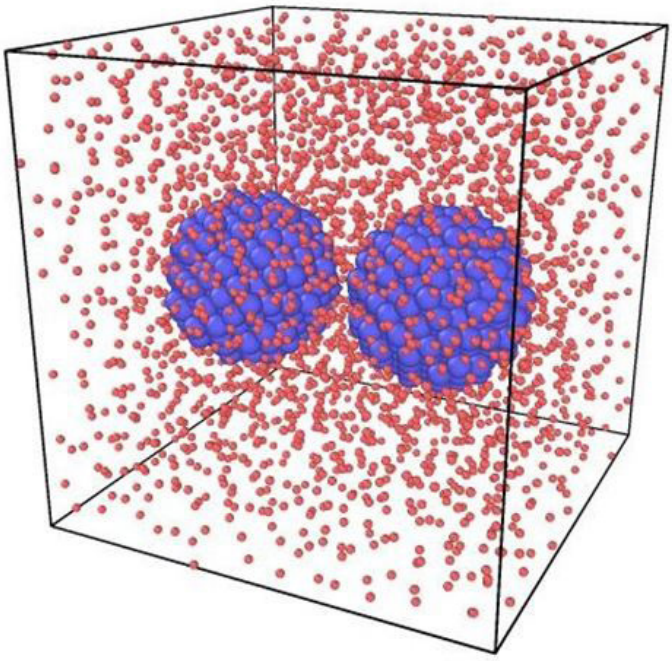

Figure 1: Snapshot of the suspension

NP Diameter, D(nm)	Atom number in a NP	Number of liquid N_2	System size (nm)	NP volume fraction (%)
2	370	4721	6.53×6.53×6.53	3
2	370	3491	5.94×5.94×5.94	4
2	370	2502	5.51×5.51×5.51	5
3	1168	8445	8.27×8.27×8.27	5
4	2899	22100	11.02×11.02×11.02	5

Table 2: Parameters of the suspension models

The radial distribution function (RDF) and the diffusion coefficient, denoted by D, are calculated to characterize the suspension. The RDF can reflect the aggregation of the particles in the system. It is the ratio of the local density to the average density, and calculated by

$$g(r) = \left(\frac{N(r)}{\Delta V(r)}\right)/\rho \quad (4)$$

where $N(r)$ represents the number of atoms in the shell of r→r+dr centered on one referenced atom, $\Delta V(r)$ is the shell volume, and ρ is the average density of the referenced atom.

Diffusion is one physical process in which the atom transports from one part to another of the system due to its random movement. The diffusion speed is characterized by *D*. In MD, *D* can be obtained by the Green-Kubo method or the Einstein method [19]. We chose the latter, and the formulas are

$$MSD = R(t) = \langle|\vec{r}(t) - \vec{r}(0)|^2\rangle \quad (5)$$

$$D = \lim_{t\to\infty} \frac{MSD}{6t} \quad (6)$$

where MSD is the mean squared displacement, ⟨… ⟩ represents the ensemble average and *t* is time.

Results and discussion

Suspension state of the NPs

The distance of the center of mass (COM) and the interaction potential energy between the NPs at the different times are calculated for the suspensions, and the corresponding results are depictednin Figure 2 to represent the evolution of the suspension and aggregation state of the NPs in the base liquid at 65K. The diameter of the NPs is deducted from the COM distance, and thus the shortest surface distance of two particles is attained. It is observed the NPs of 2, 3 and 4nm do not aggregate in the base fluid during the whole simulation process (see Figures 2a, b and c), and the obtained shortest surface distance increases with increasing the particle size. So the smaller NPs are apt to aggregate, and the larger NPs are well dispersed in the base liquid. It can be further observed from the evolution of the potential energy between two particles in the base liquid. For the suspension with the 5% NPs,

the interaction potential energy of 2nm NPs is smallest, and fluctuates around -27kcal⁄mol. In which, the negative sign indicates that the interaction force between the NPs is dominated by the attractive force. However, the potential energy of both 3nm and 4nm NPs fluctuates around 0kcal⁄mol. In the two cases, the attractive force and the repulsive force between the NPs are almost balanced. By combining the evolutions of the potential energy and the relative distance between the NPs, the nanoparticles of 4nm are found to best dispersed in the base liquid due to the largest relative surface distance, and the suspension with 3nm particles is most stable due to the smallest fluctuation of both the COM distance and the interaction potential energy after about 1ns.

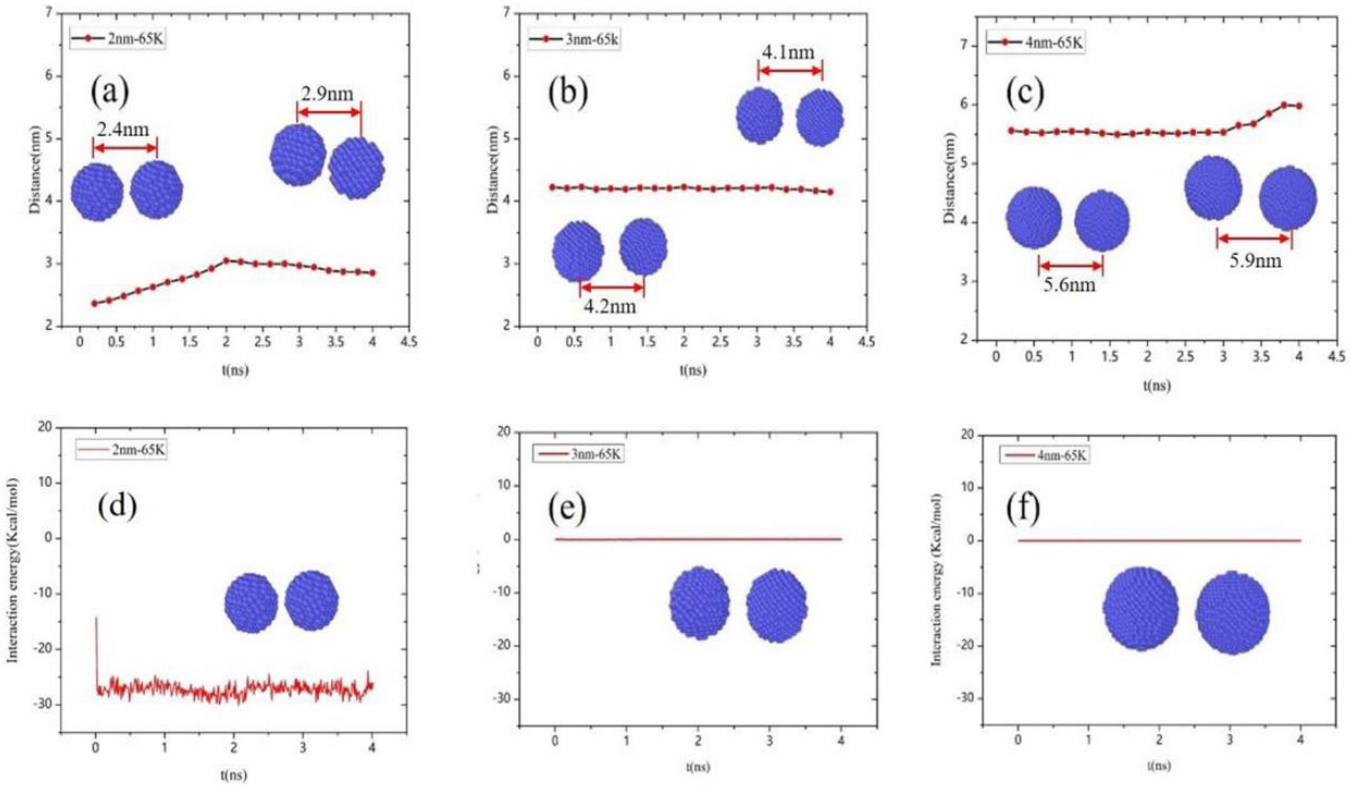

Figure 2: Evolution of the COM distance **(a-c)** and the interaction energy **(d-f)** between two particles with the different sizes

The evolution of the COM distance and the interaction potential of 2nm NPs in the suspensions at 75K, 85K, 95K and 105K are shown in Figures 3 and 4, respectively, and the case at 65K can be seen from Figures 2a and d. When the temperature rises from 65K to 75K, the shortest surface distance from about 1nm to 0nm, the interaction potential energy of 2nm NPs decreases from −27 kcal⁄mol to −364 kcal⁄mol, and the two particles aggregate. Upon rising the temperature to 85K, the shortest surface distance increases, the interaction energy fluctuates -49kcal⁄mol, and the two particles do not aggregate. When the temperature reaches to 95K, the particles aggregate again, and the interaction energy fix on the constant value of -456kcal⁄mol. Upon rising the temperature, the state and the interaction energy do not almost change. Although 2nm NPs already aggregate together at 75K, the state is unstable. Rising the temperature, the particles transit from the unstable aggregation to the disperse state to the stable aggregation. As a result, the liquid suspension is more stable at 95K or the higher temperature. It is because both the COM distance and the interaction potential energy fix at a constant value, respectively. Elevating the temperature makes the thermal movement of the whole system more acute, thereby resulting in the easier aggregation of NPs but the more stability of the liquid suspension.

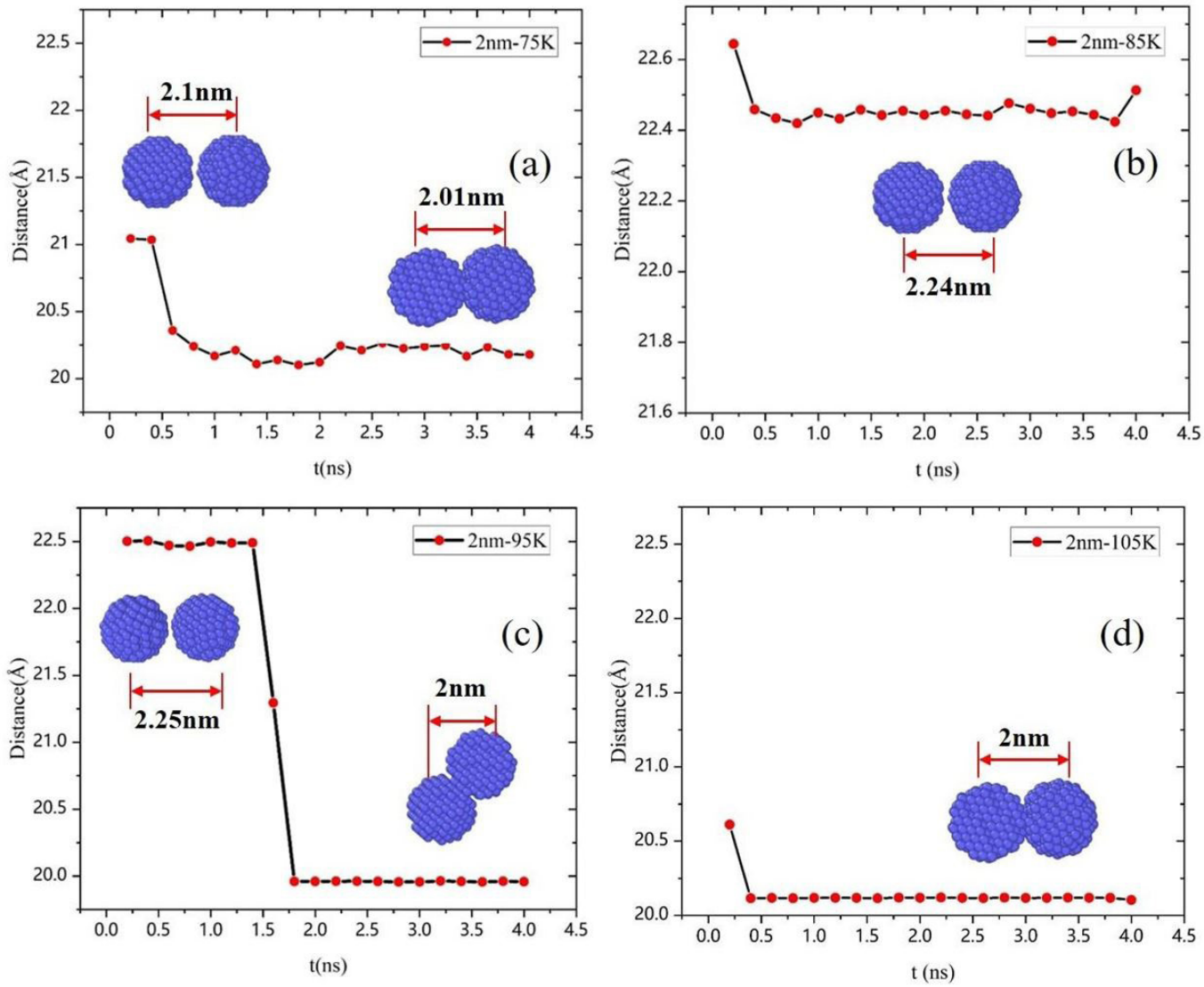

Figure 3: Evolution of the COM distance between two particles at at 75K **(a)**, 85K **(b)**, 95K **(c)**, and 105K **(d)**

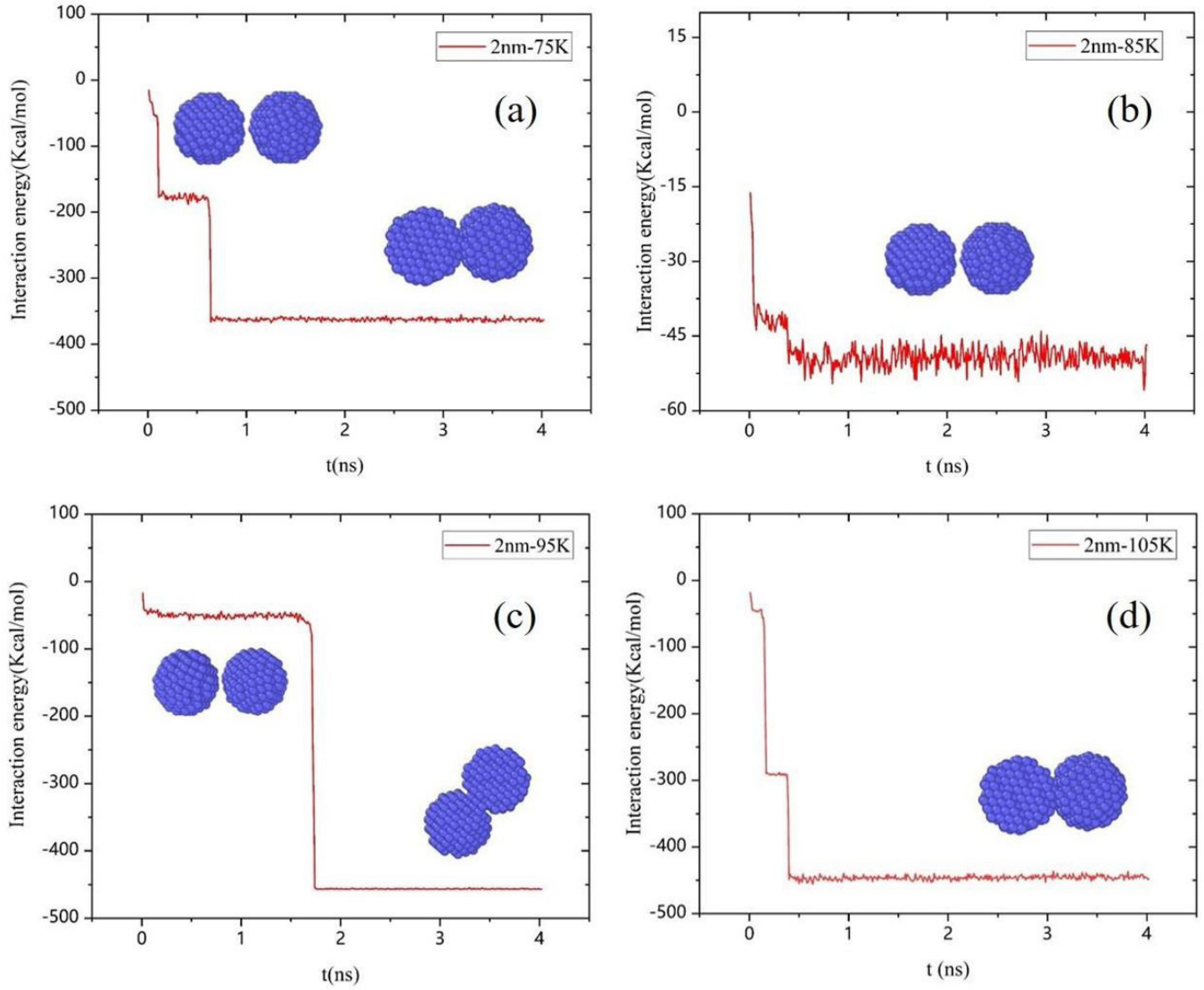

Figure 4: Evolution of the interaction energy between two particles at 75K **(a)**, 85K **(b)**, 95K **(c)** and 105K **(d)**

Radial distribution function

RDF of the base fluid

The RDFs of the pure liquid N_2 and the base liquid in the suspensions with 5% particles at 65K are represented in Figure 5. Not only the peak position is shifted toward the larger r, but the peak value decreases, when the smaller nanoparticles are suspended in the liquid N_2. However, the previous variations are not so obvious. Moreover, the N-N RDF of the suspension has the same change trend as the RDF of the pure liquid N_2. Therefore, for the considered particle volume fraction, adding the NPs does not change the space distribution of the base liquid, and the base fluid still maintains the microscopic structure characteristics of "short-range order and long-range disorder" of the liquid phase.

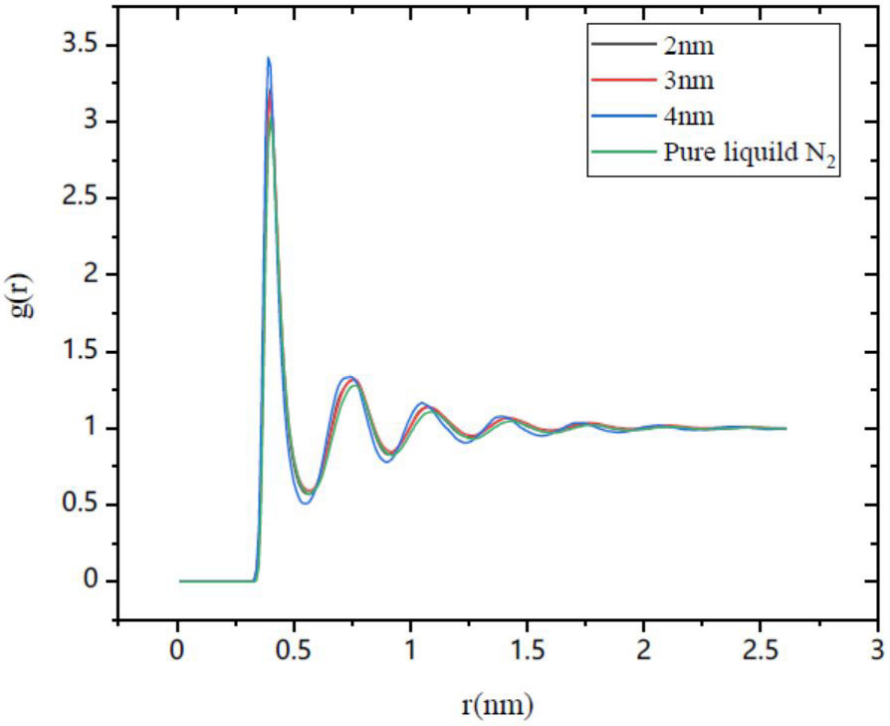

Figure 5: N-N RDFs of the different systems

RDF of the NP and base fluid

The Cu-N RDFs of the different suspensions are plotted in Figure 6. The highest peaks of the RDFs at the different temperatures are almost located at r=11.8Å (Figure 6a), and several irregular small peaks occur near the highest peak, which is resulted from several liquid layers formed around the NPs due to the strong attraction. In addition, the temperature does not almost alter the values of each peaks of the RDFs.

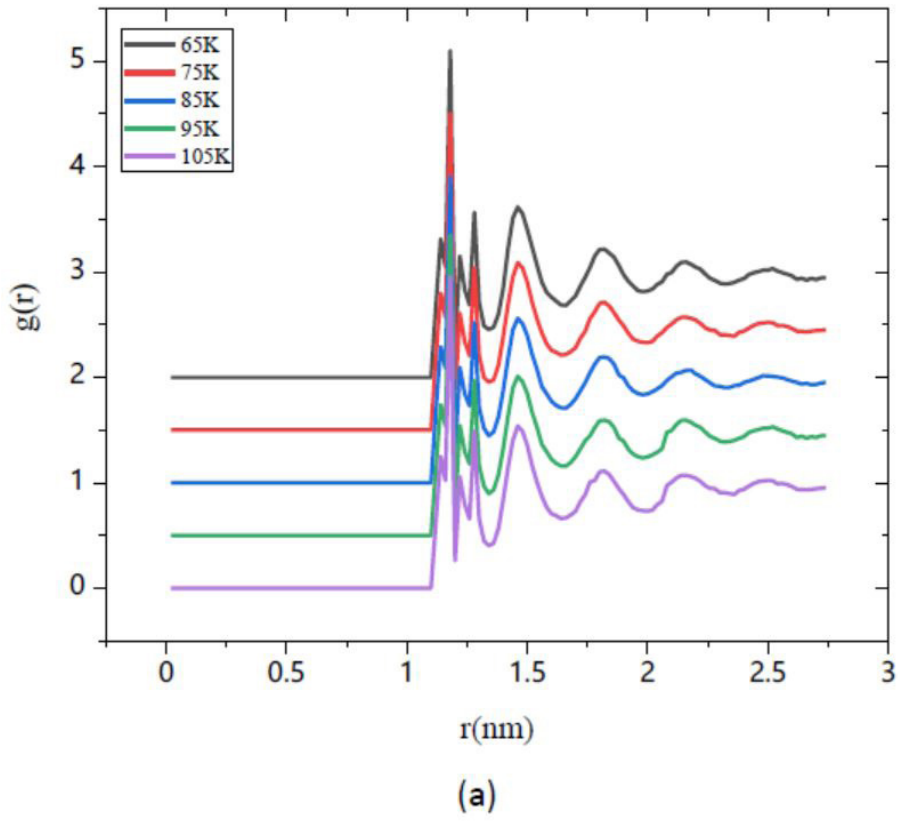

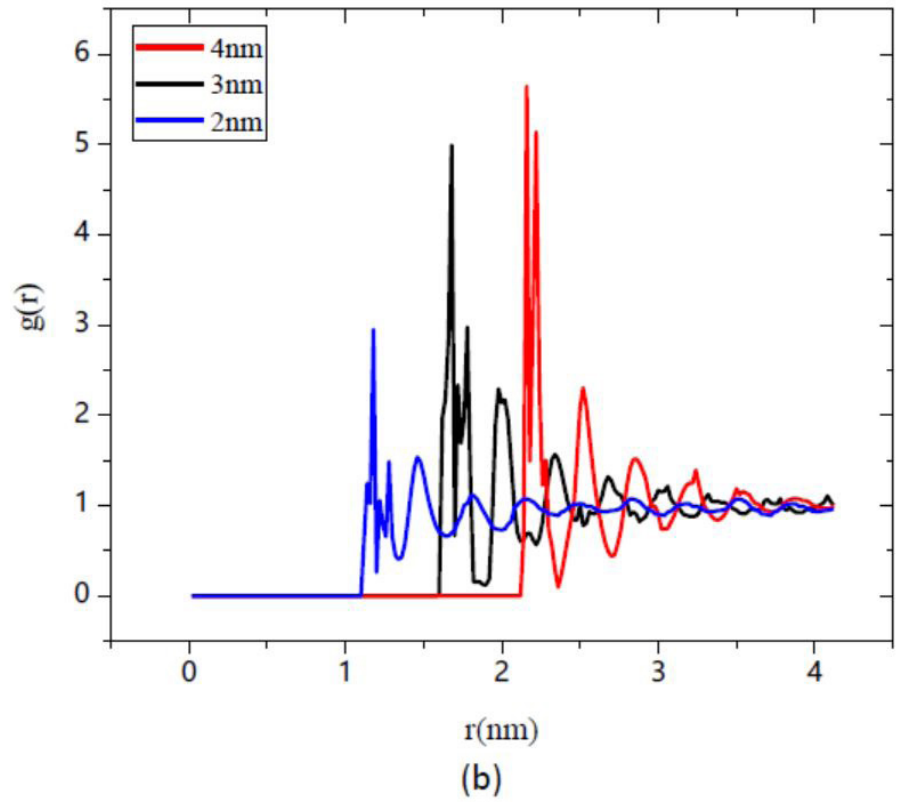

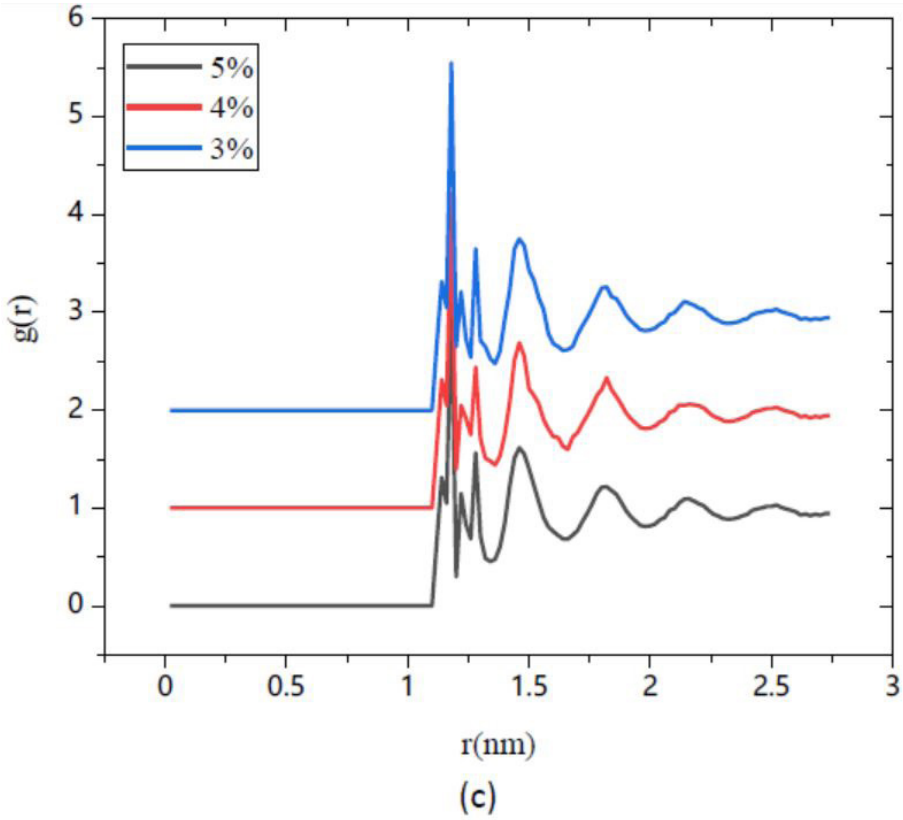

Figure 6: Cu-N RDFs of the suspensions for the different temperatures **(a)**, particle size **(b)** and volume fractions **(c)**

The Cu-N RDFs of the suspensions with 5% NPs at 65K are further depicted in Figure 6b. The highest peak appears at r=11.8Å, 16.8 Å and 21.6 Å, respectively for the suspensions with 2, 3 and 4nm NPs. Meanwhile, the values of each peak become larger for the bigger particles. So the probability of the liquid N_2 occurring near the bigger particles is larger, and the dispersion state of the

NPs In the liquid suspension is better. For the larger NP, the liquid N2 molecules are much more likely to be adsorbed around the NP due to the stronger attractive force.

The Cu-N RDFs of the suspension with the different volume fractions of 2nm particles are plotted in Figure 6c. The volume fraction of the NPs has no obvious effect on the Cu-N RDFs of the suspensions.

Diffusion

Mean square displacement

The variations of the MSD with the temperature are depicted in Figure 7 for the pure liquid N_2 and the suspensions with5% 2 nm NPs. Each MSD linearly increases with time, and enlarges with the temperature rising. It is because one larger temperature makes the Brownian motion of the atoms in the system strengthen. At a given temperature, the MSD of the pure liquid N_2 is significantly greater than the MSD of the suspension. When NPs are adding into the liquid N_2, some of them are absorbed near the NPs to form the layer structure due to the strong particle attraction. On the other hand, compared to the liquid molecules, the random movement of the NPs is relatively slow. Consequently, the MSD of the suspension becomes smaller than one of the base liquid.

The impact of the volume fraction and size of the NPs on the suspension MSDs at 65K is further given in Figure 8. The previous results show that the NP addition causes the system MSD to be decreased. However, for the given volume fraction, the larger NP requires more base fluid molecules, thereby the larger MSD of the suspension. At the same time, for the NPs with the same size, the smaller the volume fraction is, the fewer NPs are added, and the greater the suspension MSD is.

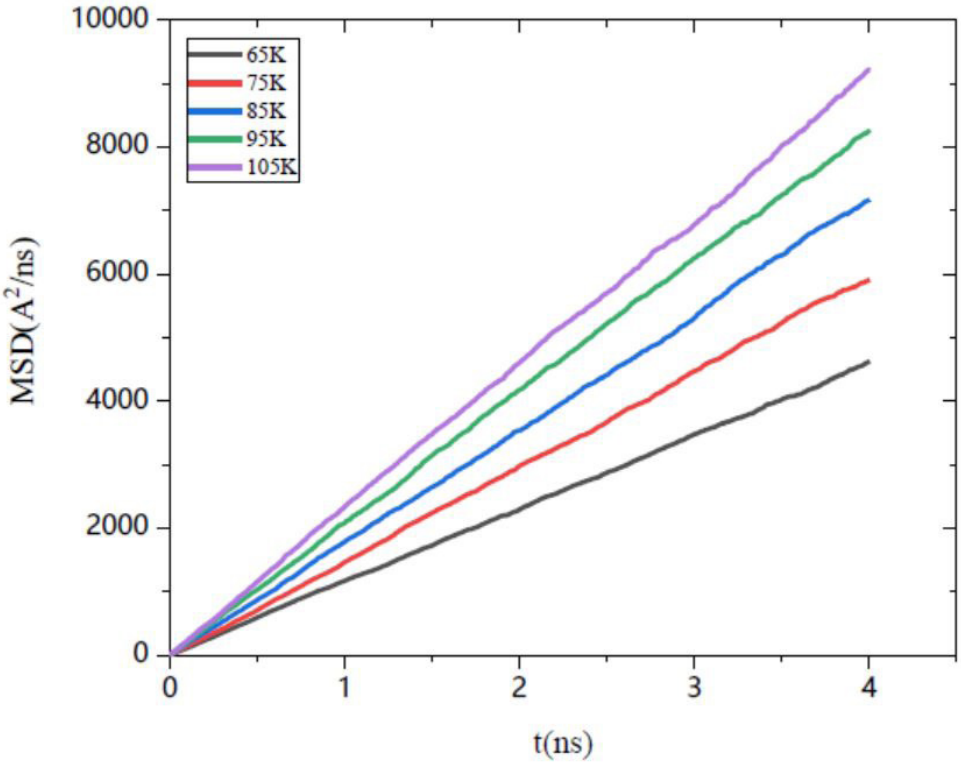

(a)

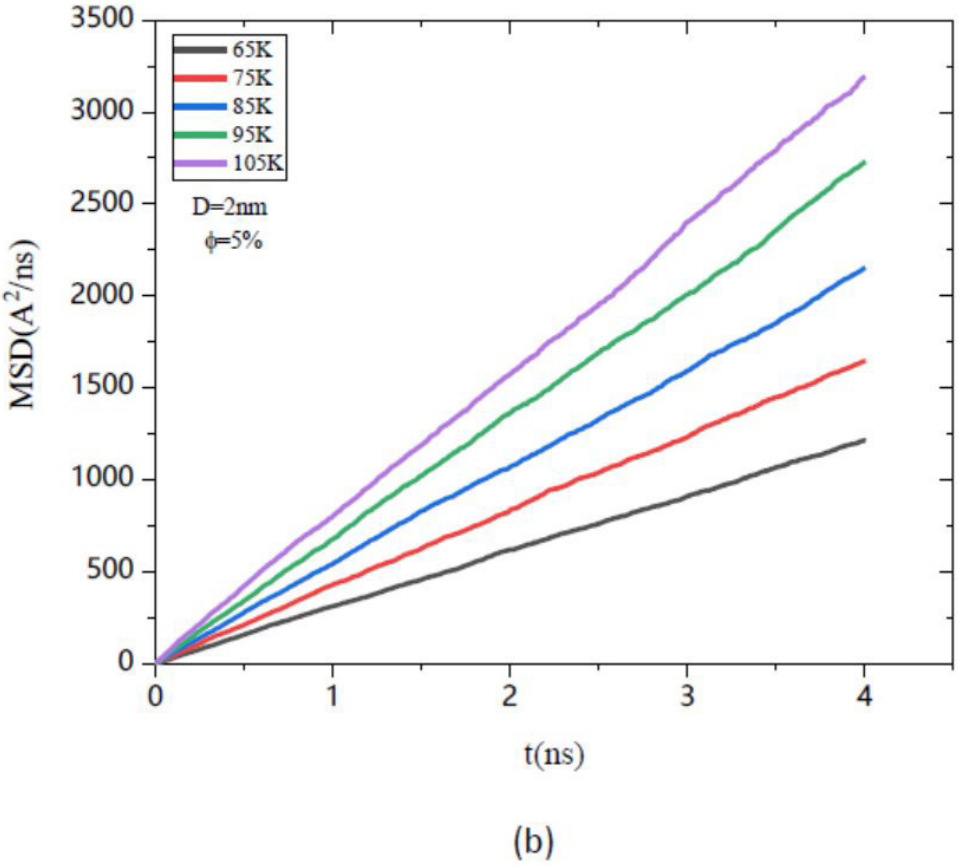

Figure 7: MSDs of the pure liquid N_2 **(a)** and the suspensions **(b)** at the different temperatures

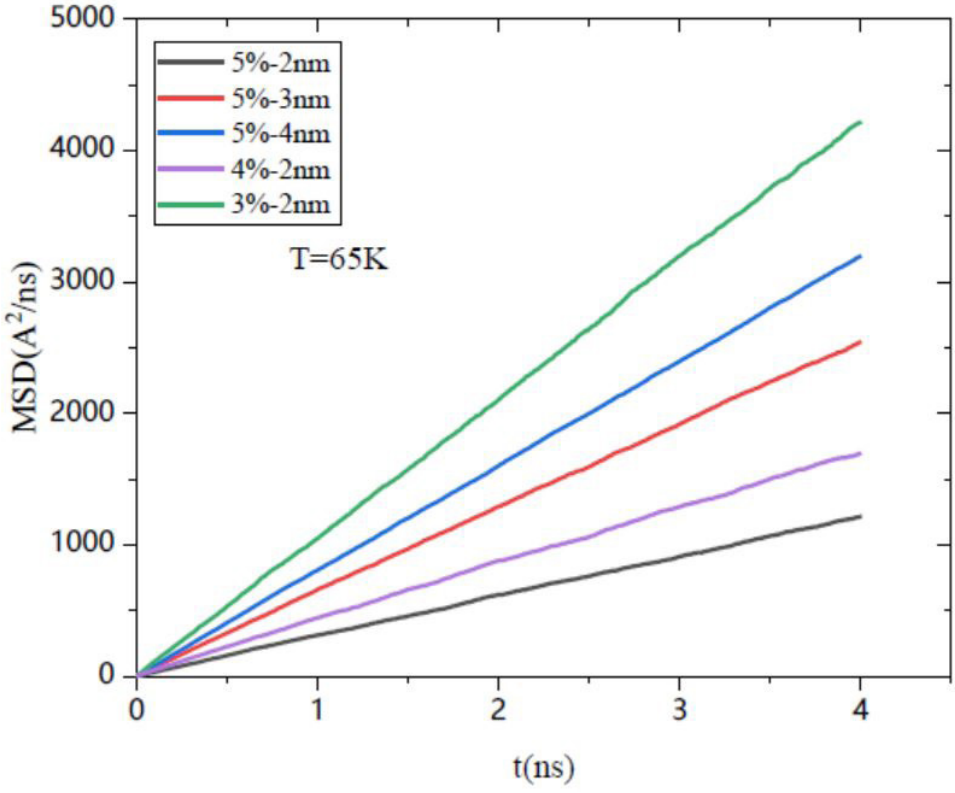

Figure 8: MSDs of the different suspension systems

Diffusive coefficient

It is known that the influence of the temperature on the diffusion coefficient is well described by the Arrhenius formula

$$D = D_0 \exp\left(-\frac{E_a}{N_A k_B T}\right) \quad (7)$$

where D_0 represents the limit value of D when the temperature approaches infinity, E_α is the activation energy of diffusion, N_A is the Avogadro's number, and k_B is the Boltzmann's constant.

Taking the natural log of both sides of Eq. (7) yields

$$\ln D = \ln D_0 - \frac{E_a}{N_A k_B T} \quad (8)$$

Therefore ln$D$ is a linear relationship with 1/T, and the slope is $-\frac{E_a}{N_a k_B}$, the intercept ln$D$.

The diffusion coefficients at the different temperatures are calculated for the pure liquid N_2 and the suspensions with the different volume fractions of 2nm NPs. The change in D with the temperature and the corresponding Arrhenius fit are given in Figure 9. All of D enhances with increasing the temperature. At a given temperature, D of the pure liquid N_2 is largest, followed by the suspension with the smaller particle volume fraction. In addition, from the fitted line of the Arrhenius formula, the diffusion activation energy and limiting diffusion coefficient of each system are attainable and listed in Table 3. Obviously, for the suspension with few 2nm particles, the less activation energy is required to diffuse, and the corresponding D0 is larger. It suggests the nanoparticles could be much better suspended in the base liquid. Therefore, for the NPs with the same size, the smaller the volume fraction is, the easier the atom diffuses, and the better the suspension degree is. It agrees with our previous results. In addition, Ea and D0 of the pure liquid N2 are smaller and larger, respectively, than the corresponding values of the suspensions with the different volume fractions of 2nm NPs.

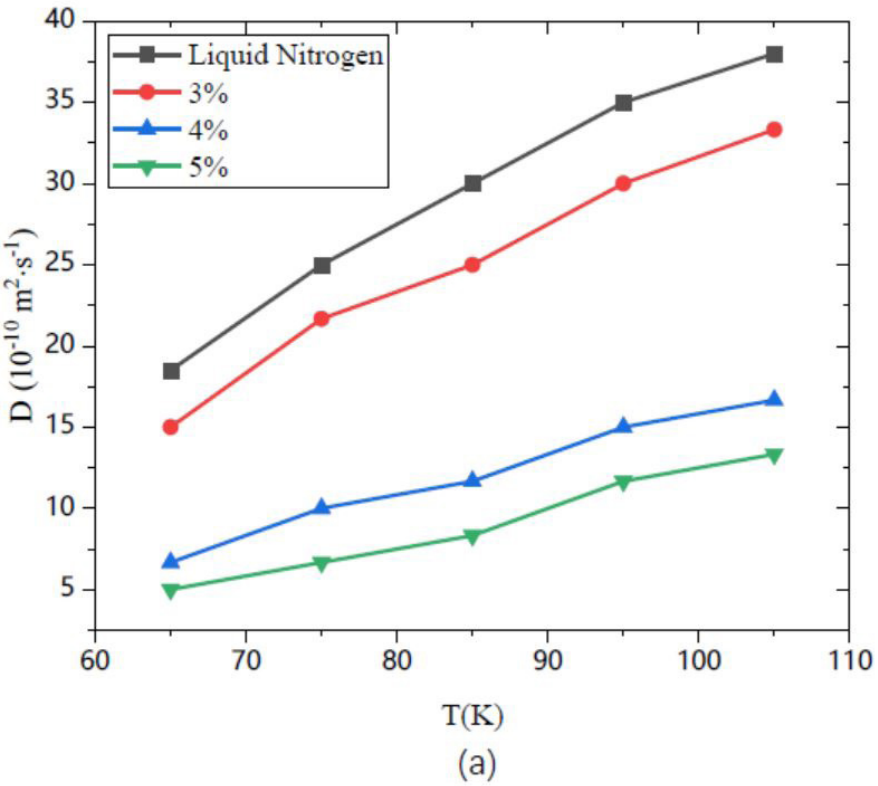

(a)

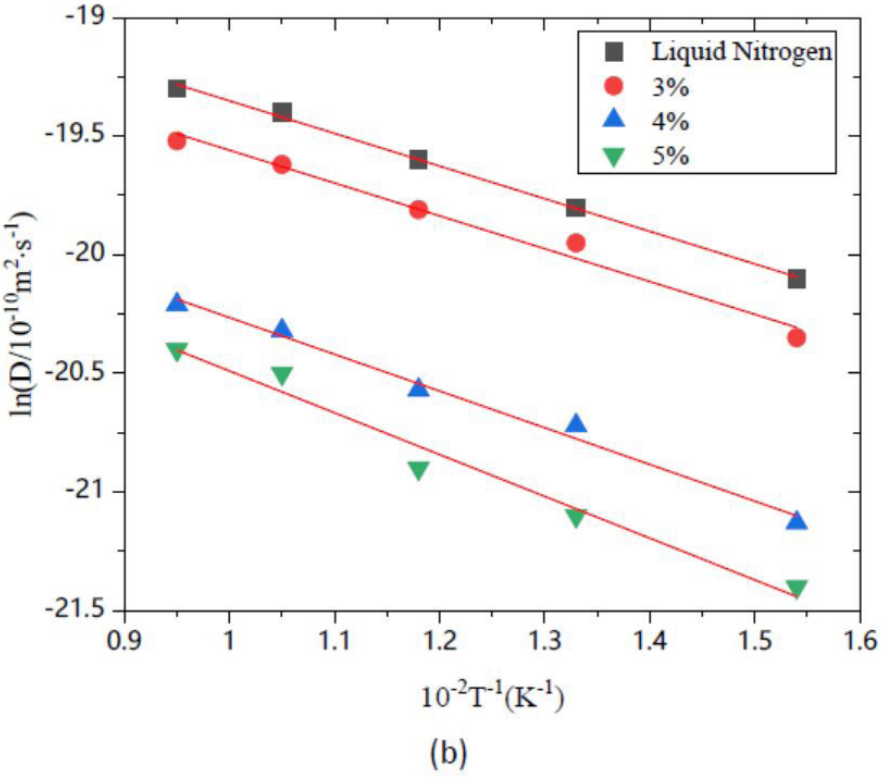

Figure 9: Diffusion coefficients **(a)** and the Arrhenius diagram **(b)** for the suspensions and the liquid N_2

Particle diameter D(nm)	Volume fraction (%)	E_α (J/mol)	D_0 (10–10m² · s⁻¹)
0	0	11.4267	156.03
2	3	11.5112	127.74
2	4	12.7554	76.44
2	5	14.6404	74.23
3	5	11.8233	89.56
4	5	9.797	81.33

Table 3: E_α and D_0 of the different systems

The effect of the particle size on D at 65K is represented in Figure 10 for the suspension with 5% NPs, and the corresponding activation energy and limit diffusion coefficients are also listed in Table 3. For the suspension with 5% NPs, *Ea* becomes smaller when the particle size increases, and even smaller than *Ea* of the liquid N2 for 4nm NPs. Meanwhile, *D0* firstly increases and then decreases as the particle diameter increases from 2 to 4nm, but still smaller than *D0* of the liquid N2. So at a given volume fraction of the NPs, the smaller NPs are easier to aggregate in the base fluid, which in turn causes the diffusion activation energy to enhance and the limit diffusivity to reduce. For the liquid suspension with 5% NPs, 3nm is the best size of the particles suspended in the base fluid.

Additionally, the Arrhenius fit becomes worse for the suspension with 2nm NPs, which is resulted from the aggregation of NPs in the base fluid.

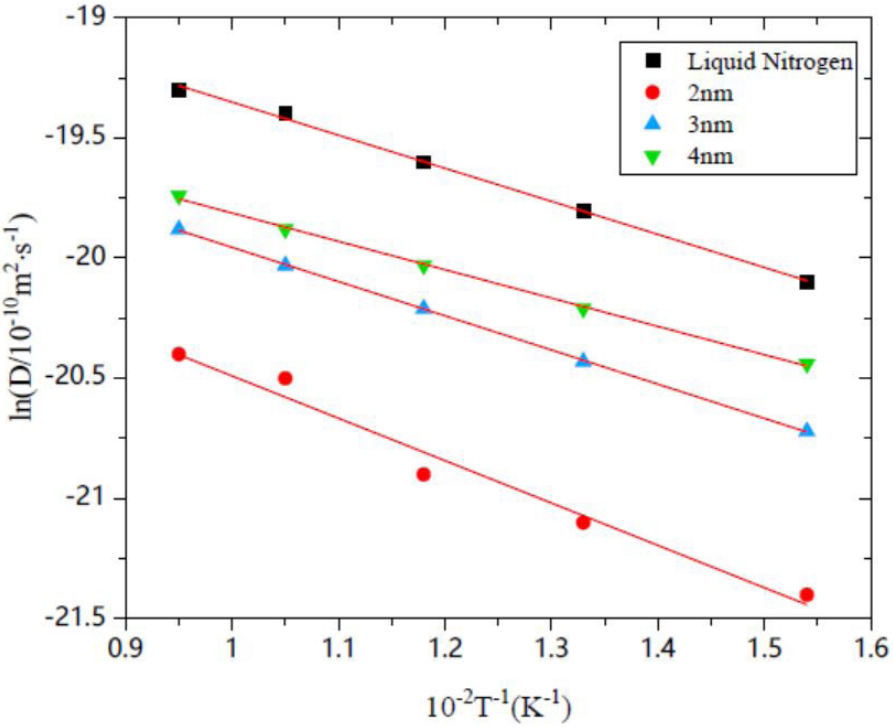

Figure 10: Arrhenius diagram for the suspensions with 5% of the different NPs

Conclusions

The larger-scale molecular dynamics simulations are performed to investigate the microscopical characteristics of liquid suspensions comprised of Cu NPs and liquid N_2 on the different conditions. The following main conclusions can be withdrawn:

1. The particle size has a significant effect on the aggregation state and suspension stability of the NPs in the liquid suspensions. At 65K and the volume fraction of 5%, the smaller particles are apt to aggregate while no aggregation. Among the particle size considered, the suspension with 3nm NPs is most stable.

2. As the temperature rises, although the aggregation degree between the NPs increases, the stability of the suspension improves, and the particles undergo the transition from the unstable aggregation to the dispersion state to the stable aggregation. For the suspension with 5% 2nm NPs, the stable state is attainable at the temperature of 95K.

3. After the NPs with the certain volume fraction added, the base fluid still presents the microscopic structural characteristics of "short-range order and long-range disorder". However, the different liquid layers are formed around the NPs. The radial distribution functions of the particle liquid molecules are considerably sensitive to the volume fraction of the particles, but not to the system temperature and the particle size.

4. The relationship between the diffusion coefficients and the temperature of the suspension is still described by the Arrhenius formula. However, the smaller size and the larger volume fraction of NPs lead to the larger errors due to the aggregation of the NPS. The diffusion coefficients of the suspension also increase with increasing the temperature. While keeping the particle size unchanged, the smaller the particle volume fraction is, and the greater the diffusion coefficient of the suspension becomes. For the suspensions with the volume fraction of 5% at 65K, 3nm is found to be the best size of the Cu NPs suspended in the liquid N2-based fluid.

Acknowledgements

This work was supported by the National Natural Science Foundation of China [grant numbers 51776027, 51906229].

References

1. Wen QL (2020) Rapid and Sensitive Electrochemical Detection of MicroRNA by Gold Nanoparticle-catalyzed Silver Enhancement. Analyst.

2. Rischitor G, Parracino M, Spina RL, Urbán P, Ojea-Jiménez I, et al. (2016) Quantification of the cellular dose and characterization of nanoparticle transport during in vitro testing. Particle and Fibre Toxicology 13: 1-47.

3. Kahani SA, Mashhadian, (2016) Preparation of bimetallic Co-Ag and Co-Cu nanoparticles by transmetallation of tetrakis (pyridine) silver(II) peroxydisulfate and tetrakis (pyridine) sulfatocopper(II) monohydrate complexes[J]. Journal of Alloys and Compounds: An Interdisciplinary. Journal of Materials Science and Solid-state Chemistry and Physics.

4. MunyaloJ M, Zhang XL (2018) Particle size effect on thermophysical properties of nanofluid and nanofluid based phase change materials: a review. Journal of Molecular Liquids 265: 77-87.

5. Liebersbach P (2020) CFD Simulations of Feeder Tube Pressure Oscillations and Prediction of Clogging in Cold Spray Nozzles. Journal of Thermal Spray Technology 29: 400-12.

6. Markus AA, Parsons JR, Roex EWM (215) Modeling aggregation and sedimentation of nanoparticles in the aquatic environment. Science of the Total Environment 506-507: 323-9.

7. Sun XM, Tabakman SM, Seo WS (2010) Separation of Nanoparticles in a Density Gradient: FeCo@C and Gold Nanocrystals. Angewandte Chemie 121: 957-60.

8. Allen MP, Tildesley DJ (1987) Computer simulations of liquids. 1987.

9. Zheng ZM, Wang BA (2018) Prediction model for the effective thermal conductivity of nanofluids considering agglomeration and the radial distribution function of nanoparticles. Acta Mechanica Sinica 34: 507-14.

10. Anoop KB, Sundararajan, Das SK (2009) Effect of particle size on the convective heat transfer in nanofluid in the developing region. International Journal of Heat and Mass Transfer 52: 2189-95.

11. Sedighi M, Mohebbi A (2014) Investigation of nanoparticle aggregation effect on thermal properties of nanofluid by a combined equilibrium and non-equilibrium molecular dynamics simulation. Journal of Molecular Liquids 197: 14-22.

12. Wang R, Qian S, Zhang Z (2018) Investigation of the aggregation morphology of nanoparticle on the thermal conductivity of nanofluid by molecular dynamics simulations. International Journal of Heat and Mass Transfer 127: 1138-46.

13. Lu J, Liu DM (2015) Molecular dynamics simulations of interfacial interactions between small nanoparticles during diffusion-limited aggregation. Applied Surface Science 2015.

14. Yang YJ, Oztekin A, Neti S, Mohapatra S (2012) Particle agglomeration and properties of nanofluids. Journal of Nanoparticle Research 14: 852.

15. Feng Y, Yu B, Feng K (2008) Thermal conductivity of nanofluids and size distribution of nanoparticles by Monte Carlo simulations. Journal of Nanoparticle Research 10: 1319-28.

16. Xu J, Yu B, Zou M (2006) A new model for heat conduction of nanofluids based on fractal distributions of nanoparticles. Journal of Physics D Applied Physics 39: 4486-90.

17. Prasher R, Evans W, Meakin P (2006) Effect of aggregation on thermal conduction in colloidal nanofluids. Applied Physics Letters 89: 143119-143119-3.

18. Xiao BQ, Yang Y, Chen LX (2013) Developing a novel form of thermal conductivity of nanofluids with Brownian motion effect by means of fractal geometry. Powder Technology 239: 409-14.

19. Toghraie D, Mokhtari M, Afrand M (2016) Molecular dynamic simulation of Copper and Platinum nanoparticles Poiseuille flow in a nanochannels. Physica E: Low-dimensional Systems and Nanostructures 84: 152-61.

20. Zou Y, Huai XL (2009) Molecular Dynamics Simulation for Homogenous Nucleation of Water and Liquid Nitrogen in Explosive Boiling. In: ASME International Mechanical Engineering Congress and Exposition 1735-40.